J Mater Sci (2007) 42:1054–1059
DOI 10.1007/s10853-006-0964-0

LETTER

# Low-temperature solid-state synthesis and phase-controlling studies of CdS nanoparticles

**Jinsong Liu · Jieming Cao · Ziquan Li · Guangbin Ji · Shaogao Deng · Mingbo Zheng**

Received: 6 March 2006 / Accepted: 11 September 2006 / Published online: 12 January 2007


## Introduction

In recent years, intensive development of nanocrystalline materials in nanotechnology has occurred worldwide. CdS has been an important semiconductor owing to its unique electronic and optical properties, and its potential applications in solar energy conversion, nonlinear optical, photoelectrochemical cells and heterogeneous photocatalysis [1, 2]. To date, synthesis of nanosized CdS has been a subject matter of immense interest and its synthesis has been tried by various methods [3–14]. However, either complex process control, reagents or long synthesis time would be required for these routes.

Recently, solid-state reaction has been developed in the synthesis of nanomaterials due to its many advantages: no need for solvent, no pollution, simple process and so on [15–21]. Though CdS nanoparticles have also been synthesized by room temperature solid-state reaction [22], further studies about the particles growth have scarcely been reported. Herein, we report on the further growth studies of high quality CdS nanoparticles synthesized by a simple low-temperature solid-state reaction. Different surfactants have been introduced to the reaction process, and different sizes of CdS nanoparticles have been obtained under different reaction temperatures.

J. Liu · J. Cao (✉) · Z. Li · G. Ji · S. Deng · M. Zheng
College of Material Science and Technology, Nanomaterials Research Institute, Nanjing University of Aeronautics and Astronautics, Nanjing, Jiangsu 210016, P.R. China
e-mail: jmcao@nuaa.edu.cn

Also, CdS has two different crystal patterns, which are cubic and hexagonal, respectively. As we know, cubic CdS is considered a metastable phase while hexagonal CdS is the thermodynamics stable one of the semiconductor. Usually it was believed that the phase transition process of CdS from cubic to hexagonal would be happened under high temperature or microwave radiation [23], and the research on this transition process has been reported [24]. In this paper, it was found that crystal patterns of CdS nanoparticles would be easily controlled by the suitable surfactant or addition, and this phase-controlling could be carried out in low-temperature solid-state reaction, which is very interesting and simple.

## Experimental

### Chemicals

The cadmium acetate (AR) $Cd(CH_3COO)_2 \cdot 2H_2O$, thioacetamide (AR) $CH_3CSNH_2$, Ionic Liquids: $[C_2OHmim][Cl]$ (a new series $[C_nO_mmim][X]$ of imidazolium cation-based room temperature ionic liquids), $[C_4H_9mim][Cl]$ (1-*n*-alkyl-3-methylimidazolium $[C_nmim][X]$ series room temperature ionic liquids) (prepared according to literature [25]) and P123 (poly-(ethylene glycol)-block-poly-(propylene glycol)-block-poly-(ethylene glycol)). All chemicals were directly used without special treatments.

### Sample preparation

Different synthesis processes were employed as follows. Procedure I, 2.67 g (0.01 mol) of $Cd(CH_3COO)_2 \cdot 2H_2O$

was ground for 5 min before mixed with 0.75 g (0.01 mol) $CH_3CSNH_2$. After the mixture was ground for 10 min in an agate mortar, it was heated for 1 h at 60 °C in an oven. The product was washed for several times with distilled water. Finally the obtained solid was dried in air at 60 °C for 5 h, and marked as sample A1. The processes of procedure II and III were similar to the procedure I except the different heating temperatures of 120 °C and 180 °C in ovens, and the as-prepared products were marked as A2 and A3, respectively. Procedure IV, 2.67 g (0.01 mol) of $Cd(CH_3COO)_2 \cdot 2H_2O$ was ground for 5 min before it was mixed with 3 mL [$C_2$OHmim][Cl]. After 3 min of grinding, 0.01 mol $CH_3CSNH_2$ was added to the mixture. Then the mixture was heated for 1 h at 60 °C in an oven after ground for 5 min. The product was washed for several times with distilled water. Finally the solid was dried in air at 60 °C for 5 h, and marked as sample A4. Procedure V, 4.00 g P123 was used instead of 3 mL [$C_2$OHmim][Cl], other process was same as procedure IV and the product was marked as A5.

## Apparatus

X-ray powder diffraction (XRD) was carried out on a Bruker D8-Advance X-ray diffractometer with CuK$\alpha$ radiation ($\lambda$ = 0.154178 nm). Transmission electron microscopy (TEM) micrographs and selected-area electron diffraction (SAED) patterns were taken using a FEI Tecnai-20 transmission electron microscope, with an accelerating voltage of 200 kV. After completion of the reaction, TEM samples were prepared by placing a drop of the dilute ethanol solution on the surface of a copper grid (250 mesh), and UV–vis absorption spectra were recorded on an Hp-6010 spectrometer with the samples dispersed in alcohol at room temperature.

## Results and discussion

The X-ray diffraction patterns for the various products of CdS are shown in Fig. 1. The patterns of A1, A2, A3 and A5 are compared with the data of the JCPDS File No. 89-0440 and are in good agreement with that of pure cubic phase of CdS. The three pronounced peaks with $2\theta$ = 26.5, 43.7 and 52.0° correspond to the three crystal plans of (111), (220) and (311) of CdS cubic phase, respectively. The dimensions of the CdS nanoparticles calculated from the widths of the major diffraction peaks observed in Fig. 1 through the Scherrer formula are listed in Table 1. As shown in Table 1, the FWHM value is getting smaller and smaller with the increasing of heating temperature, which implies the increasing of CdS particles size. From Table 1, we could also find that particles diameter of A5 is smaller than that of A1. It is thought that P123 slowed the growth process of the particles, which can control the size of nanoparticles.

However, the reflection peaks of CdS in the pattern of A4, (100), (002), (101), (102), (110), (103), (112), appear at $2\theta$ = 24.9, 26.7, 28.2, 36.7, 43.7, 47.9 and 51.9°, respectively. These results indicate that it has a hexagonal structure, which is obviously different from other samples. So the utility of [$C_2$OHmim][Cl] has an important effect on the crystal pattern of the CdS nanoparticles. The dimension of the CdS nanoparticles calculated from the widths of (103) diffraction peak through the Scherrer formula is 5.27 nm.

Therefore, to further ascertain function of [$C_2$OHmim][Cl] in the phase-controlling process of CdS, extra experiments have been designed to explore the process: 3 mL [$C_2$OHmim][Cl] was substituted of 1 mL [$C_2$OHmim][Cl], 2 mL [$C_2$OHmim][Cl], 1 mL [$C_4H_9$mim][Cl] and 3 mL [$C_4H_9$mim][Cl] in the solid-state reactions, and the samples obtained were marked as B1, B2, B3 and B4, respectively.

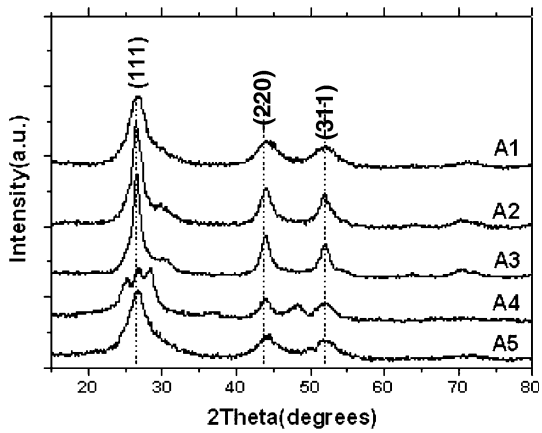


**Fig. 1** XRD patterns of the samples obtained by low-temperature solid-state reaction

**Table 1** Crystallite sizes along (111), (220) and (311) zone axes

| Sample | Particle sizes (nm) calculated from (111), (220) and (311) plans | | | Average sizes (nm) |
|---|---|---|---|---|
| A1 | 2.96 | 3.16 | 3.09 | 3.07 |
| A2 | 5.10 | 4.73 | 5.01 | 4.95 |
| A3 | 6.60 | 6.09 | 5.73 | 6.14 |
| A5 | 2.58 | 3.22 | 3.12 | 2.97 |

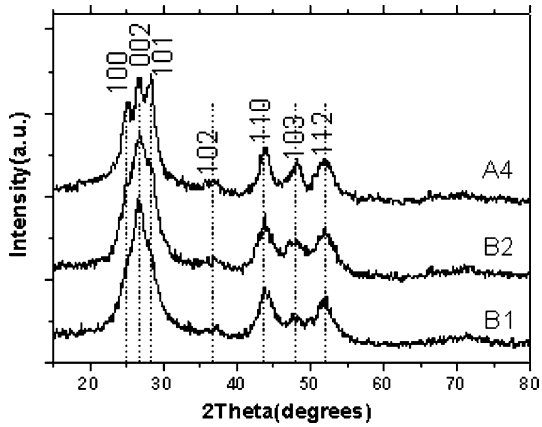


**Fig. 2** XRD patterns of B1, B2 and A4 obtained by low-temperature solid-state reaction

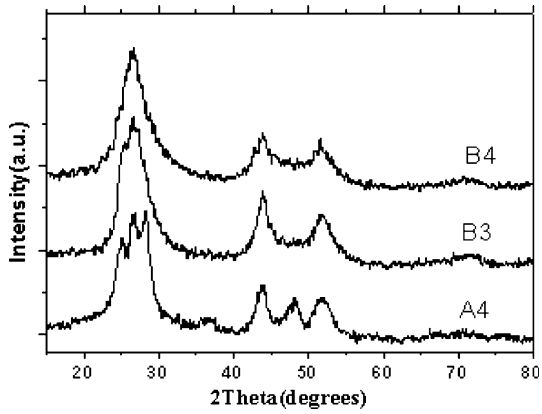


**Fig. 3** XRD patterns of B3, B4 and A4 obtained by low-temperature solid-state reaction

The effect of the volumes of $[C_2OHmim][Cl]$ on the products has been investigated. Figure 2 shows the XRD patterns of B1, B2 and A4 obtained in the conditions of different volumes. There are weak peaks at 36.7° and 47.9° in XRD pattern of B1, which are the characteristic peaks of hexagonal CdS. It indicates that hexagonal CdS is being formed after addition of a small quantity of $[C_2OHmim][Cl]$, though it is not still crystallized well. It can be also seen from this figure that intensities of the diffraction peaks in crystal plates $(10a)$ $[a = 0, 1, 2, 3]$ are getting stronger and stronger as the increase of $[C_2OHmim][Cl]$ volumes. The diffraction peaks of A4 display distinct hexagonal crystal structure with the higher crystalline than B1 and B2. From these experiments, we can conclude that the addition of $[C_2OHmim][Cl]$ could only change $S^{2-}$ ions arrangement at the beginning of solid-state reaction, leading to the formation of hexagonal phase. Volume of $[C_2OHmim][Cl]$ could only play an important role on the crystallization process of the products, and it is the most suitable concentration to form well crystallized hexagonal CdS nanoparticles in solid-state reaction when the addition of $[C_2OHmim][Cl]$ is 3 mL.

Figure 3 shows the XRD patterns of A4, B3 and B4 when using $[C_4H_9mim][Cl]$ instead of $[C_2OHmim][Cl]$. It can be seen that B3 and B4 are in great agreement with the cubic CdS with the diffraction peaks of 26.5, 43.7 and 52.0°, while pronounced diffraction peaks at $2\theta = 24.9$, 28.2, 36.7 and 47.9°, which are distinct characteristic peaks of hexagonal CdS nanoparticles, shows the hexagonal crystal structure of A4. Addition of $[C_4H_9mim][Cl]$ could not change the CdS crystal pattern, and $S^{2-}$ kept face-center cube arrangement, resulting in the final cube structure. In addition, for B3 and B4, FWHM (Full Width at Half Maximum) from the diffraction peak at 26.5° is different ($FWHM_{B4} > FWHM_{B3}$), it shows that particles sizes of cubic CdS get smaller as increasing of $[C_4H_9mim][Cl]$ Volume. The cation $[C_4H_9mim]^+$ could not control crystal pattern, and $[C_2OHmim]^+$ is considered to be a key factor in the formation process of hexagonal CdS nanoparticles.

Figure 4 shows the TEM micrograph of A4. This micrograph indicates that the CdS nanoparticles consistently show crystal structure with unchanging morphology. The typical morphology of the CdS is small spheres with the average diameter of about 5 nm, which is in agreement with the XRD result. The agglomeration of particles in TEM may be arisen from the small dimensions and high surface energy. The SAED pattern shows multicrystal structure of the CdS nanoparticles. TEM images of other samples are almost the same as A4 except the different diameters of the particles

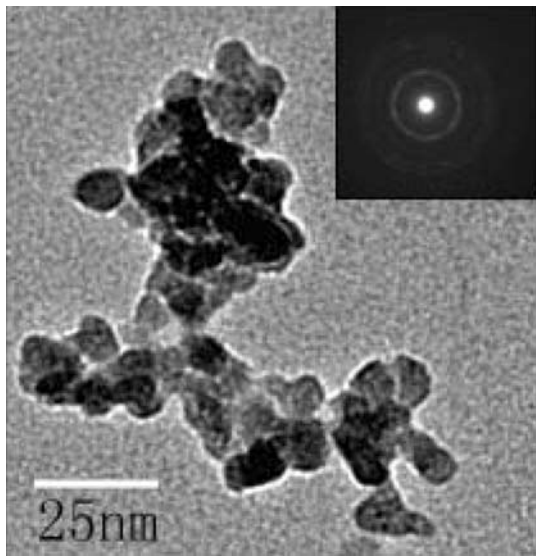


**Fig. 4** TEM micrograph and SAED pattern of A4 obtained by low-temperature solid-state reaction

(shown in Fig. 5), and the dimensions of A1–A3 and A5 observed from TEM images are in the range of 2.5–3.5, 4.5–6.0, 5.5–7.0 and 2.0–3.5 nm, respectively, which are in agreement with the XRD results. As is well known, particle size distribution is an important feature of powders. In this paper, the particles size could be faciley controlled by selecting different temperatures and the addition of surfactants.

In general, absorption spectra probe the crystallite internal molecular orbital and provide information concerning size and particle composition [21]. Optical absorption spectra for CdS ethanol solutions are presented in Fig. 6. As shown in the Fig. 6, the spectra exhibit distinct exciton absorption, and we can observe that UV–vis optical absorption excitonic peaks of the CdS nanoparticles are at 465, 489, 495, 448 and 456 nm corresponding to A1, A2, A3, A4 and A5, respectively. The corresponding band gap energy of absorption maximum for all the samples could be determined using the equation:

$$E_g = h \cdot c/\lambda_{max} \quad (1)$$

The bandgaps of A1, A2, A3, A4 and A5 calculated are 2.66, 2.53, 2.51, 2.76 and 2.71 eV, respectively. Compared with the peak of bulk CdS (510 nm, 2.42 eV) crystals [5], it shows obvious blue shift, which clearly indicates the presence of quantum-size effects in the as-prepared CdS nanoparticles.

Compared to A1, A2 and A3, it can be seen that the excitonic absorption peaks gradually red shift as the particle sizes increase, and it can be noted that the absorbance at the peak maximum is practically temperature-dependent. However, when P123 was added to the solid-state reaction (A5), the peak would shift to the shorter wavelengths, which implies that the smaller size of nanoparticles were obtained in the presence of P123.

It is also very interesting that value of the absorption peak is smaller than others, and shows stronger blue shift when using [$C_2$OHmim][Cl] as the additive (A4), which may arise from the different phase of CdS obtained. It provides a simple approach to obtain hexagonal CdS with strong absorption, through many properties are unknown at the phase transition from cubic to hexagonal. The size of the nanoparticles could be calculated from the band gap values by using the effective mass approximation [26]. This method has been proved to be reliable for sizes larger than 4 nm [27]. The nanoparticles size is obtained by using the following formula:

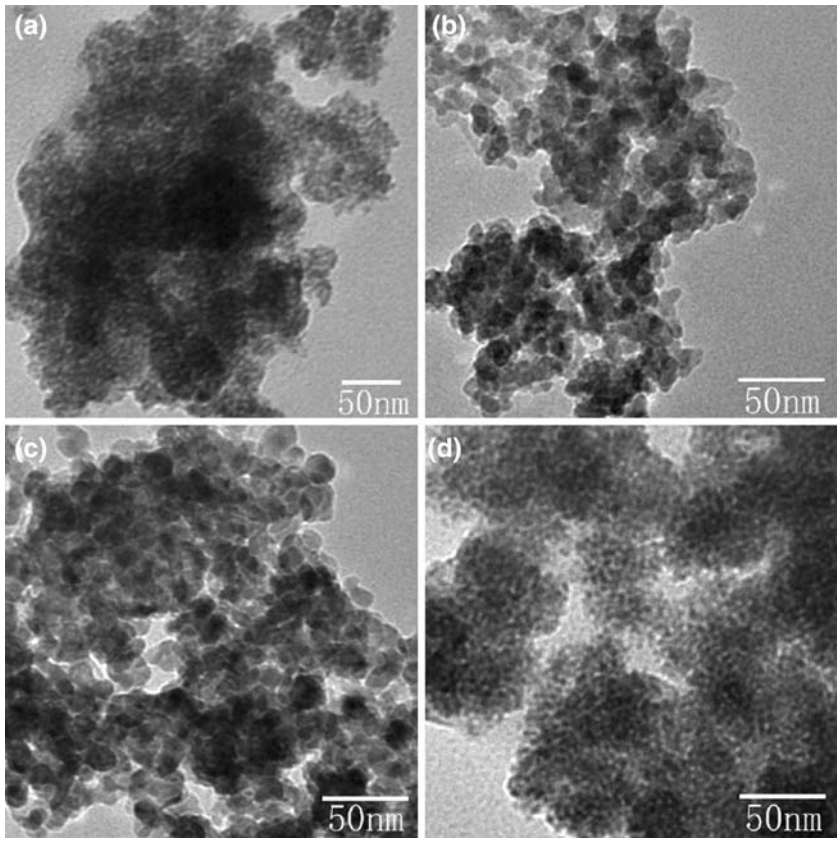


**Fig. 5** TEM images of (**a**) A1, (**b**) A2, (**c**) A3 and (**d**) A5 obtained by low-temperature solid-state reaction

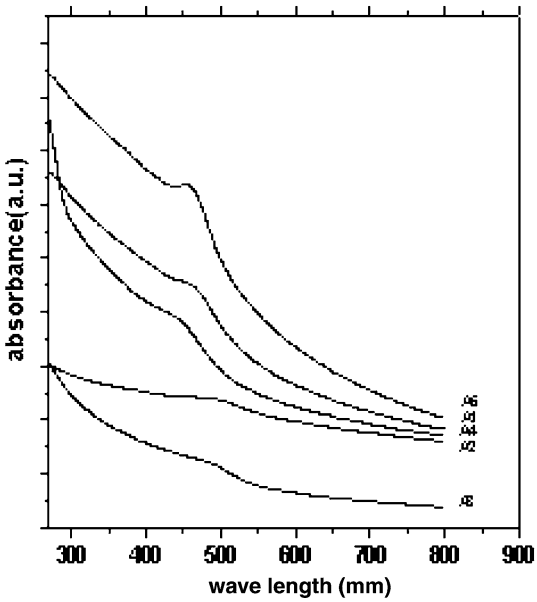


**Fig. 6** UV–vis spectra of the samples obtained by low-temperature solid-state reaction

$$E_g = E_{g0} + \frac{h^2\pi^2}{2R^2}\left[\frac{1}{m_e^*} + \frac{1}{m_h^*}\right] - \frac{1.8e^2}{\varepsilon R}$$

where $R$ is the nanoparticles radius and $m_e^*$ and $m_h^*$ are the effective mass of electron and hole in the lattice. The values for $m_e^*$ and $m_h^*$ are 0.2 $m_e$ and 0.7 $m_e$, respectively. The size of A4 estimated from the optical band gap values is about 5.2 nm, which is in good accordance with the size determined from the transmission electron microscopy studies. In addition, from the Fig. 6 it can be also observed that there are tails of more intense absorption occurring at shorter wavelengths which are due to higher energy electronic transitions as observable in low band gap semiconductor nanoparticles [28].

It is well known that the chemical reaction is always composed of four stages, which are diffusion, reaction, nucleation and growth [15]. In general, it is thought that the evolution of CdS nanoparticles is influenced by the kinetic mechanism and the growth process is controlled by diffusion. In this paper, the sizes of cubic CdS nanoparticles could be controlled by the temperature of solid-state reaction in the absence of surfactant. Cubic CdS nanoparticles are formed when $Cd^{2+}$ ions fill the tetrahedral clearance of $S^{2-}$ face-center cube that is first formed in the process of solid-state reaction. After P123 is added to the reaction, it does not act with $S^{2-}$ ions. The experiment result shows that P123 only prevents the particles from growing up, leading to obtaining less size of nanoparticles. However, when $[C_2OHmim][Cl]$ is added to the solid-state reaction, $[C_2OHmim]^-$ will act with $S^{2-}$ ions, and change their arrangement, and result to the formation of $S^{2-}$ ions hexagon arrangement [29]. Then $Cd^{2+}$ ions fill the tetrahedral clearance of $S^{2-}$ hexagon, resulting to the formation of hexagonal CdS nanoparticles. While $[C_4H_9mim]^-$ could only act the same influence as P123, and control the size of particles, and could not change the crystal pattern of CdS. The results give us a fast, simple and novel way to synthesize different crystal patterns of CdS nanomaterials with different properties. The more detailed study of formation mechanism of different crystal patterns will be described in progress.

## Conclusions

Growth studies of high quality CdS nanoparticles have been investigated by low-temperature solid-state reaction. The sizes of CdS nanoparticles can be controlled by heating temperatures and surfactants. The crystal patterns would be influenced by the surfactants. TEM and XRD technologies were used to characterize the CdS nanoparticles. By optical properties measurements, the absorption peaks of CdS show strong blue shift from that of the bulk. Detailed phase-controlling process between cubic and hexagonal CdS has also been studied by further experiments, and $[C_2OHmim]^+$ is considered to be a key factor in the formation process of hexagonal CdS nanoparticles.

**Acknowledgement** This work has been supported by the doctor Innovation Funds of Nanjing University of Aeronautics and Astronautics (BCXJ05-07).

## References

1. Hu K, Brust M, Bard AJ (1998) Chem Mater 10:1160
2. Weller H (1993) Angew Chem Int Ed 32:41
3. Tamborra M, Striccoli M, Comparelli R, Curri ML, Petrella A, Agostiano A (2004) Nanotechnology 15:240
4. Khiew PS, Huang NM, Radiman S, Ahmad MS (2004) Mater Lett 58:516
5. Ludolph B, Malik MA, Obrien P, Revaprasadu N (1998) Chem Commun 17:1849
6. Uosaki K, Okamura M, Ebina K (2004) Faraday Discuss 125:39
7. Khanna PK, Lonkar SP, Subbarao VVVS, Jun KW (2004) Mater Chem Phys 87:49
8. Ren T, Xu JZ, Tu YF, Xu S, Zhu JJ (2005) Electrochem Commun 7:5
9. Li Y, Huang FZ, Zhang QM, Gu ZN (2000) J Mater Sci 35:5933

10. Curri ML, Leo G, Alvisi M, Agostiano A, Della Monica M, Vasanelli L (2001) J Colloid Inter Sci 243:165
11. Xu W, Akins DL (2004) Mater Lett 58:2623
12. Wei QL, Kang SZ, Mu J (2004) Colloids Sur A: Physicochem Eng Aspects 247:125
13. Torimoto T, Yamashita M, Kuwabata S, Sakata T, Mori H, Yoneyama H (1999) J Phys Chem B 103:8799
14. Hirai T, Okubo H, Komasawa I (2000) J Mater Chem 10:2592
15. Zhou YM, Xin XQ (1999) Chinese J Inorg Chem 15:273
16. Kanade KG, Hawaldar RR, Pasricha R, Radhakrishnan S, Seth T, Mulik UP, Kale BB, Amalnerkar DP (2005) Mater Lett 59:554
17. Jin CF, Yuan X, Ge WW, Hong JM, Xin XQ (2003) Nanotechnology 14:667
18. Liu Q, Ni YH, Yin G, Hong JM, Xu Z (2005) Mater Chem Phys 89:379
19. Chen CN, Zhu CL, Hao LY, Hu Y, Chen ZY (2004) Chem Lett 33:898
20. Zhou TY, Xin XQ (2004) Nanotechnology 15:534
21. Wang ZJ, Zhang HM, Zhang LG, Yuan JS, Yan SG, Wang CY (2003) Nanotechnology 14:11
22. Wang WZ, Liu ZH, Zheng CL, Xu CK, Liu YK, Wang GH (2003) Mater Lett 57:2755
23. Cao JM, Fang BQ, Liu JS, Chang SQ, Zhang F (2005) Chinese J Inorg Chem 21:105
24. Zelaya-Angel O, Castillo-Alvarado F de L, Avendailo-Lopez J, Escamilla-Esquivel A, Contreras-Puente G, Lozada-Morales R, Torres-Delgadod G (1997) Solid State Commun 104:161
25. Branco LC, Rosa JN, Moura Ramos JJ, Afonso CAM (2002) Chem Eur J 8:3671
26. Caponetti E, Pedone L, Chillura Martino D, Panto V, Liveri VT (2003) Mater Sci Engineer C 23:531
27. Taghavinia N, Iraji-zad A, Mohammad Mahdavi S, Rezaesmaili M (2005) Phys E 30:114
28. Calandra P, Longo A, Liveri VT (2003) J Phys Chem B 107:25
29. Huaxue W, Chemistry Office of Dalian University of Technology, Higher Education Publishing Company, p 346